



Review

Young Investigator Award

A wild-derived inbred mouse strain, MSM/Ms, provides insights into novel skin tumor susceptibility genes

Kazuhiro OKUMURA, Megumi SAITO and Yuichi WAKABAYASHI

Department of Cancer Genome Center, Division of Experimental Animal Research, Chiba Cancer Center Research Institute, 666-2 Nitonacho Chuo-ku, Chiba 260-8717, Japan

Abstract: Cancer is one of the most catastrophic human genetic diseases. Experimental animal cancer models are essential for gaining insights into the complex interactions of different cells and genes in tumor initiation, promotion, and progression. Mouse models have been extensively used to analyze the genetic basis of cancer susceptibility. They have led to the identification of multiple loci that confer, either alone or in specific combinations, an increased susceptibility to cancer, some of which have direct translatability to human cancer. Additionally, wild-derived inbred mouse strains are an advantageous reservoir of novel genetic polymorphisms of cancer susceptibility genes, because of the evolutionary divergence between wild and classical inbred strains. Here, we review mapped *Stmm* (skin tumor modifier of MSM) loci using a Japanese wild-derived inbred mouse strain, MSM/Ms, and describe recent advances in our knowledge of the genes responsible for *Stmm* loci in the 7,12-dimethylbenz(a)anthracene (DMBA)/12-O-tetradecanoylphorbol-13-acetate (TPA) two-stage skin carcinogenesis model.

Key words: 7,12-dimethylbenz(a)anthracene (DMBA)/12-O-tetradecanoylphorbol-13-acetate (TPA) two-stage skin carcinogenesis, MSM/Ms, skin tumor susceptibility gene, *Stmm* loci, wild-derived inbred mouse strain

Introduction

Identifying specific genetic variants responsible for increased susceptibility to familial or sporadic cancers has significant implications for predicting individual cancer risk and developing strategies for prevention or targeted therapy [1, 2]. Mouse models of cancer have been extensively used to analyze the genetic basis of cancer susceptibility and have led to the identification of multiple loci that confer, either alone or in specific combinations, an increased susceptibility to cancer [3–8].

One of the most commonly used experimental inflammatory cancer models is the DMBA/TPA two-stage skin carcinogenesis model. The pathology of this model is almost identical to that of human skin cancer, and it offers an ideal model to research skin cancer initiation and growth [9, 10]. The first step is to treat mice with a

low dose of the mutagenic substance 7,12-dimethylbenz(a)anthracene (DMBA) to initiate carcinogenesis. In the second step, mice are continuously treated with 12-O-tetradecanoylphorbol-13-acetate (TPA) to stimulate epidermal tumor growth. During tumor promotion, papillomas are thought to be caused by an inflammatory response owing to additional TPA treatment. After long-term treatment (approximately 20 weeks), some benign tumors (papillomas) progressed to squamous cell carcinoma (SCC; Fig. 1). The role of various genes and cellular signaling pathways involved in developing skin tumors can be investigated in this two-stage skin carcinogenesis model by using a genetically engineered mouse model [10]. Genetically modified mice have been used to analyze various genes (i.e., oncogenic transcription factors, constitutive centromere-related network proteins) [11–15].

(Received 19 January 2021 / Accepted 19 February 2021 / Published online in J-STAGE 26 March 2021)

Corresponding authors: K. Okumura. e-mail: kokumura@chiba-cc.jp

Y. Wakabayashi. e-mail: yuichi_wakabayashi@chiba-cc.jp



This is an open-access article distributed under the terms of the Creative Commons Attribution Non-Commercial No Derivatives (by-nc-nd) License <<http://creativecommons.org/licenses/by-nc-nd/4.0/>>.

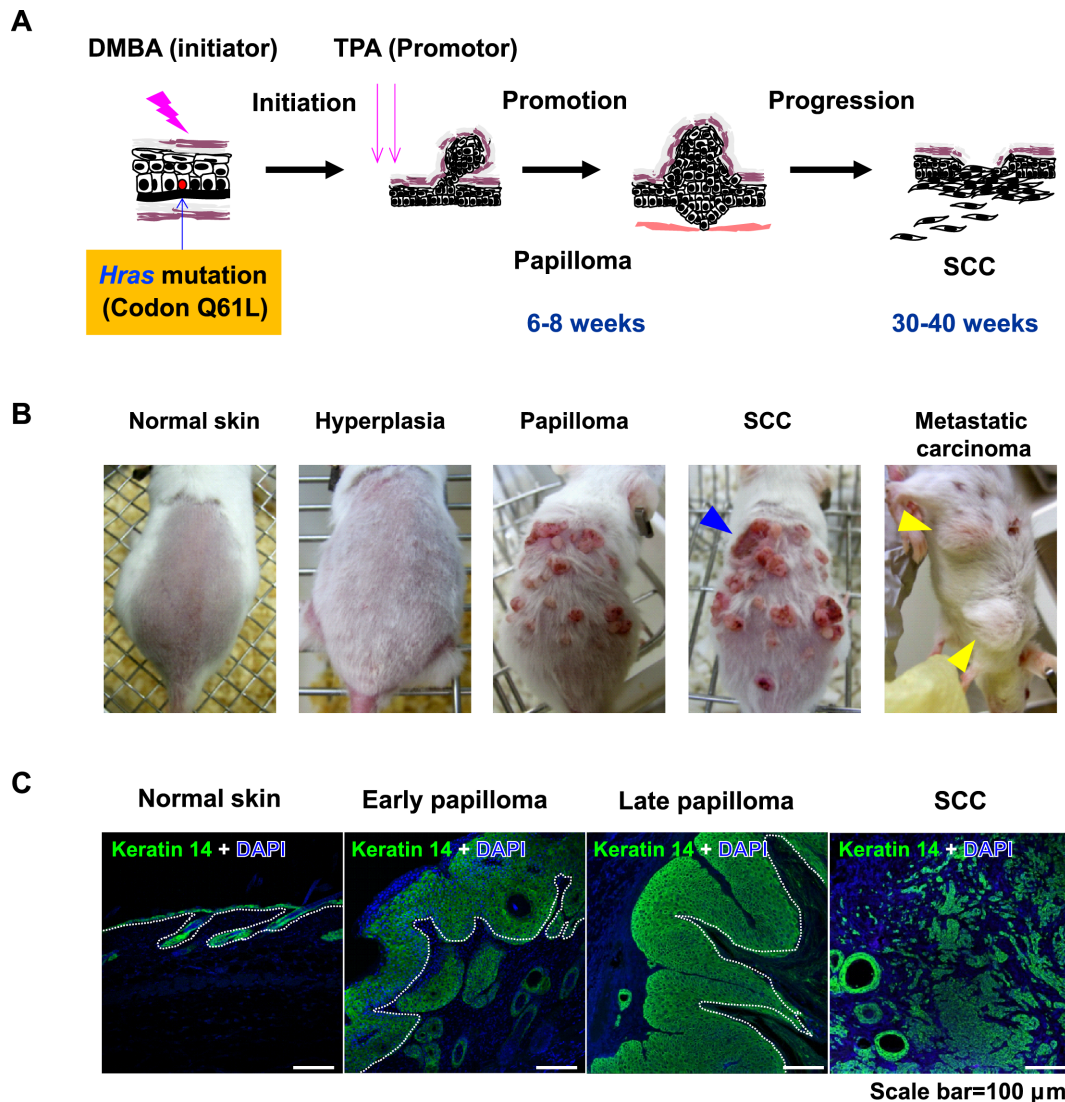


Fig. 1. 7,12-dimethylbenz(a)anthracene (DMBA)/12-*O*-tetradecanoylphorbol-13-acetate (TPA) two-stage skin carcinogenesis. (A) Topical application of the mutagenic substance DMBA at the start induces mutations in epidermal stem cell target genes. Repeated topical application of TPA begins two weeks after initiation and continues up to 20 weeks. Papillomas to develop after about eight weeks of promotion, and some tumors begin to transition to squamous cell carcinoma (SCC) after about 20 weeks. (B) Representative photographs of normal skin, hyperplastic skin, papilloma, and SCC of the dorsal back are shown. The blue arrowhead indicates an SCC. Yellow arrowheads indicate metastatic carcinomas. (C) Lower panels show immunohistochemistry-stained sections in developing chemical-induced skin tumors. Green signals indicate keratin 14 (epidermal cell marker). Blue signals indicate nuclei. Scale bar=100 μ m.

Inbred strains recently obtained from wild-derived mice are often more resistant to carcinogens and some pathogens than commonly used inbred strains. Compared with classical inbred strains, wild-derived mice show genetic polymorphisms every 100–200 base pairs in the genome [16]. Investigating the molecular basis of these traits provides insights into how polymorphisms contribute to cancer susceptibility. Most wild-derived strains reproduce with classic inbred mice, representing a rich source of evolutionarily significant diversity for forward genetics studies [16, 17]. Although still mostly unexplored, these mice are the new models for identifying

and studying novel cancer susceptibility genes. In addition, these models can be combined with the latest innovations in next-generation sequencing and genome editing technologies to study single nucleotide polymorphism (SNP) levels in cancer susceptibility genes.

Here, we review mapped *Stmm* (skin tumor modifier of MSM) loci using a Japanese wild-derived inbred mouse strain, MSM/Ms, and describe recent advances in our knowledge of the genes responsible for *Stmm* loci in the DMBA/TPA two-stage skin carcinogenesis model.

Mapping of *Stmm* Loci Using a Forward Genetics Approach

The tumor susceptibility of the DMBA/TPA two-stage skin carcinogenesis model varies among mouse strains, and a genetic approach has been employed to identify genes related to tumor susceptibility [18, 19]. Using the genetic approach, several skin tumor-susceptibility loci were identified using commonly inbred strains or wild-derived strains [20–30], some of which have clear translatability to human cancer susceptibility [31–33]. Therefore, the DMBA/TPA skin carcinogenesis model is a useful model for identifying modifier genes.

The MSM/Ms mouse strain was generated in Mishima, Shizuoka, Japan, from wild-caught mice of the *Mus musculus molossinus* subspecies [34]. Breeding for the MSM/Ms strain began in 1978, after six mice were donated to the Cytogenetics Department of the National Institute of Genetics. After repeated sister-brother mating for the past 40 years, inbreeding has reached generation N100, and these mice are now recognized as an inbred mouse strain like other commonly inbred mouse strains. Due to its genetic divergence from standard inbred mouse strains mainly established from *M. m. domesticus*, MSM/Ms has been broadly used in linkage studies, mainly in Japan. The MSM/Ms strain is also useful as a genetic resource, with complete genome sequence information (<https://molossinus.brc.riken.jp/mogplus/#JF1>) [35, 36], a full set of mouse consomic strains (MSM/Ms as the chromosome donor and C57BL/6J as the host strain) [37], a BAC clone library (https://dna.brc.riken.jp/en/cloneeseten/msm_bac_en) [38], a microsatellite database (<https://shigen.nig.ac.jp/mouse/mmdbj/top.jsp>) [39], and ES cells [40, 41] now available. In addition, MSM/Ms mice have a very low incidence of development of several types of tumors [42–45], age-dependent hearing loss [46–50], and unique behavioral traits such as a very high locomotor activity [51–56], compared with classical inbred mice.

We first investigated DMBA/TPA skin carcinogenesis using MSM/Ms and FVB/N mice as susceptible strains. In these experiments, MSM/Ms and (FVB/N × MSM/Ms) F₁ mice showed strong resistance to skin carcinogenesis, and their phenotype was dominant [57]. Therefore, in order to identify the tumor susceptibility modifier gene, we used the following protocol. 1) Using *p53* tumor suppressor gene knockout mice, we created F₁ backcross mouse groups of *p53* wild-type (*p53*^{+/+}) and heterozygous knockout mice (*p53*^{+/-}). We also investigated the dependence of the loci on the *p53* gene. 2) We made linkage analysis possible at each stage of carcinogenesis by measuring the diameters of all developing

tumors over time. Combining these improvements, 228 F₁ backcross mice (121 with the *p53*^{+/+} background and 107 with the *p53*^{+/-} background) were subjected to the DMBA/TPA chemical carcinogenesis protocol (Fig. 2). The number of papillomas at 20 weeks and the presence of carcinoma at 40 weeks were recorded in each mouse. Additionally, papillomas were further categorized into three groups based on size (<2 mm, 2–6 mm, and >6 mm in diameter; Fig. 2). All mice were genotyped using 107 SNP markers distributed evenly throughout the genome.

In a population of 228 F₁ backcross mice, highly significant QTLs for papilloma development with a maximum LOD score of 7.0 were mapped to chromosomes 7 and 4. A suggestive QTL for carcinoma development was mapped to chromosome 5. We conducted linkage analysis for each of the three categories of tumors, which were specified based on tumor diameter. As a result of linkage analysis, *Stmm1* and *Stmm2* were mapped around 50 cM of chromosome 7 as resistance loci for early and mid-stage papillomas (diameter <2 mm, 2–6 mm). We succeeded in mapping *Stmm3* as resistance to late-stage papillomas (>6 mm) locus around 40 cM on chromosome 4. Notably, *Stmm3* was not detected by linkage analysis of the F₁ group of *p53*^{+/-}, suggesting that the gene responsible for *Stmm3* is strongly dependent on the *p53* gene. We succeeded in mapping *Stmm1*–*Stmm12* on mouse chromosomes, including the less effective loci (Table 1). Previously identified cancer susceptibility loci, including other types of cancer, are also present in these candidate regions (Table 1). Further studies will be necessary to narrow down the candidate regions, by combining this information with human GWAS data and congenic mapping.

Refinement of Candidate Regions for *Stmm* Loci by Congenic Mapping

On the other hand, for *Stmm1a/b* and *Stmm3*, multiple congenic mouse strains were prepared, and mapping was performed to narrow down the candidate regions [58, 59]. We screened stage-specific papilloma modifier loci based on size (Table 1). *Stmm1* and *Stmm2* were identified on chromosome 7 as modifier loci conferring resistance to smaller-sized papillomas. Nagase *et al.* mapped the loci of *Skts1* and *Skts2* loci, which had previously been identified using a wild-derived inbred mouse strain, *Mus spretus* [25, 26]. Congenic analysis narrowed down the candidate genetic region of *Skts1* to approximately 15 Mb, which is proximal to *Igflr* [70].

Stmm2, identified near *Skts2* and *Hras* on chromosome 7, has the same effect on the allelic specificity of the *Hras* mutation as *Skts2*, suggesting that the same gene

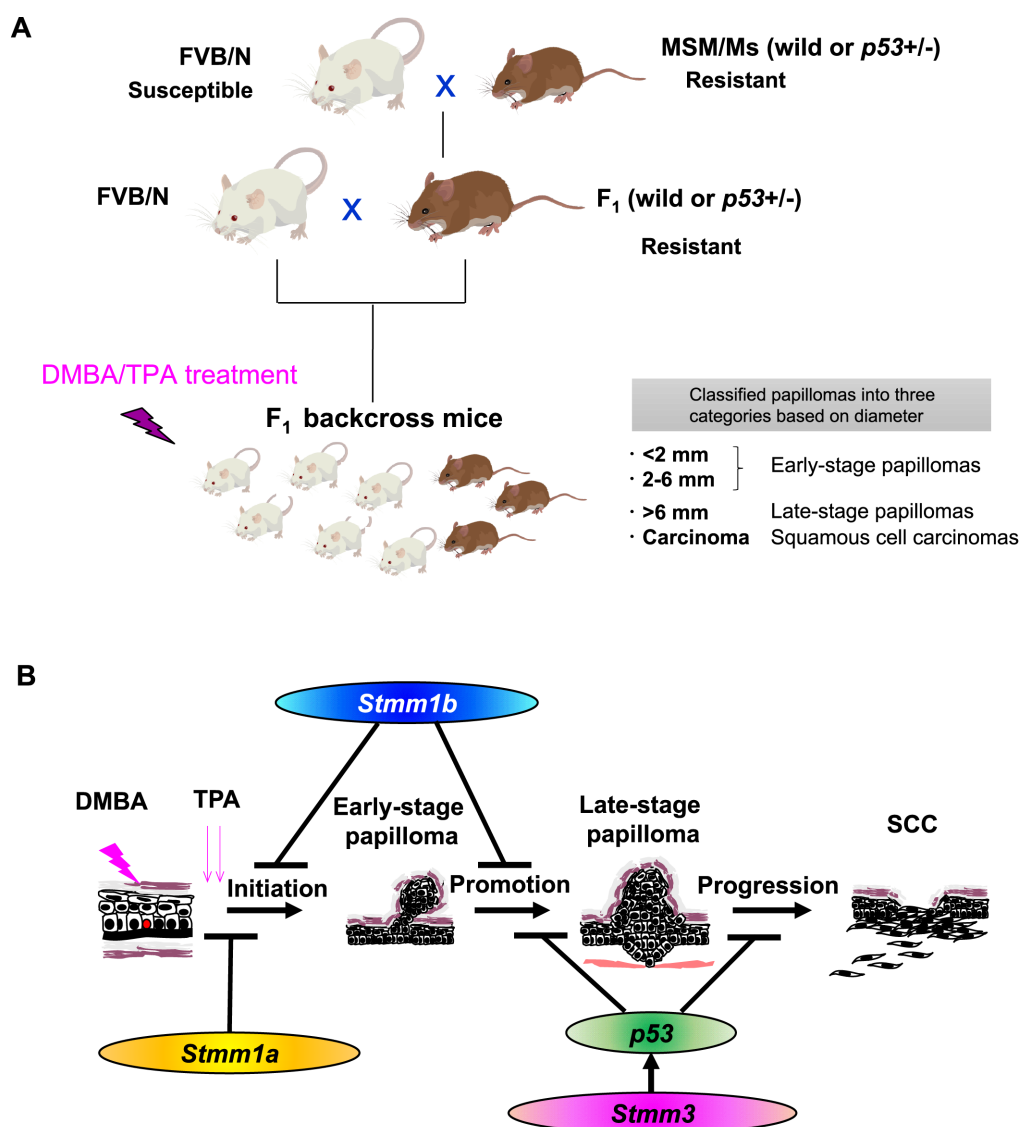


Fig. 2. Investigation of the *Stmm* loci by the forward genetics approach. (A) To identify genetic loci that control susceptibility to skin carcinogenesis, we subjected 228 FVB/N \times (FVB/N \times MSM/Ms) F₁ backcross mice, 121 on a *p53*^{+/+} background and 107 on a *p53*^{+/-} background, to the 7,12-dimethylbenz(a)anthracene (DMBA)/12-*O*-tetradecanoylphorbol-13-acetate (TPA) chemical carcinogenesis protocol. We monitored their tumor development for 40 weeks. For each mouse, we documented the number of papillomas at 20 weeks after initiation as well as the presence of carcinomas at 40 weeks. In addition, papillomas were further categorized into three groups based on size (<2 mm, 2–6 mm and >6 mm in diameter). (B) A schematic drawing of suppressive functions of *Stmm* loci in the development of a chemically induced skin tumor. *Stmm1a* is the most effective and is involved in resistance to early-stage papilloma genesis. *Stmm1b* affects papilloma formation from early to late stages, and *Stmm3* is involved in *p53* gene-dependent resistance to the malignant transformation from late-stage papillomas to squamous cell carcinomas (SCCs).

may be responsible for *Skts2* and *Stmm2* [58]. Skin carcinogenesis experiments using congenic mice with *Skts2* have not yet been reported; data presented in our report suggest that *Stmm2* and *Skts2* genes may have a relatively mild effect on papilloma multiplicity compared with *Stmm1* [58].

As previously shown, the vicinity of the *Stmm3* candidate region contains several tumor modifier loci, including *Skts7* and *Skts-fp1*, mapped for chemically induced skin papilloma susceptibility by analysis of an

NIH and *Mus spretus* cross and an FVB/N and PWK cross, respectively [23, 25] (Table 1). PWK, *Mus spretus*, and MSM/Ms are wild-derived inbred strains that share common haplotypes. A gene common to *Stmm3* might be involved in the susceptibility of these two strains through mating.

Eventually, *Stmm1* on chromosome 7 was subdivided into *Stmm1a* (about 0.24 Mb) [unpublished data] and *Stmm1b* (about 4.7 Mb) [59]. In the case of *Stmm3* on chromosome 4, the candidate region was narrowed down

Table 1. Genetic candidate regions of *Stmm* loci and other cancer susceptibility loci in the vicinity

Locus name	Chromosome No.	Genetic marker	rs No.	Candidate region [#] (bp)	Tumor category	Effect of p53	Other cancer susceptibility QTLs in the vicinity	References
<i>Stmm1a</i>	7	D7Mit351–D7Mit149	–	96,776,254–99,188,960	Early papilloma	Independent	-	[57], Okumura et al. (Unpublished data)
<i>Stmm1b</i>	7	D7Mit53–D7Mit253	–	110,583,818–115,356,689	Early-middle papilloma	Independent	-	[57–59]
<i>Stmm2</i>	7	D7Mit255–D7Mit259	–	124,705,587–144,566,894	Early-middle papilloma	Independent	<i>Skts2</i>	[25, 26, 57, 58]
<i>Stmm3</i>	4	D4Mit26–D4Mit166	–	88,535,066–93,366,888	Late papilloma, SCC	Dependent	<i>Skts7</i> , <i>Skts-fp1</i>	[22, 25, 57, 60, 61]
<i>Stmm4</i>	6	D6SNP511–D6SNP511512	rs30149679–rs38226370	55,547,013–108,360,689	Middle papilloma	Independent	<i>Skts11</i>	[25, 57]
<i>Stmm5</i>	5	D5SNP12–D5SNP6	rs13478361–rs3023057	83,810,839–126,154,436	Middle-late papilloma, SCC	Dependent	<i>Hcs5</i> , <i>Thyls2</i>	[57, 62, 63]
<i>Stmm6</i>	3	D3SNP519*	rs46831546	45,778,132 ± 10,000,000	Middle papilloma	Unknown	-	[57]
<i>Stmm7</i>	3	D3SNP504*	rs30553837	111,903,098 ± 20,000,000	Middle papilloma	Unknown	<i>Raml2</i>	[57, 64]
<i>Stmm8</i>	12	D12SNP12*	rs3682985	70,353,327 ± 20,000,000	Middle papilloma	Unknown	<i>Par3</i>	[57, 65]
<i>Stmm9</i>	13	D13SNP12*	rs3698421	71,839,279 ± 20,000,000	Middle papilloma	Unknown	<i>Pas10</i>	[57, 66]
<i>Stmm10</i>	17	D17SNP19–D17SNP510	rs3705342–N.D.	68,392,183–94,100,159	Middle papilloma	Unknown	<i>Skts10</i>	[25, 57]
<i>Stmm11</i>	11	D11SNP8*	rs3023316	117,028,591 ± 15,000,000	Middle-late papilloma, SCC	Unknown	<i>Par1</i>	[57, 67, 68]
<i>Stmm12</i>	1	D1SNP11–D1SNP512	rs3688428–rs38697954	4,137,358–32,741,433	Early papilloma	Unknown	<i>Lsccl</i>	[57, 69]

Early papilloma, tumor diameter of <2 mm; middle papilloma, tumor diameter of 2–6 mm; late papilloma, tumor diameter of >6 mm; SCC, squamous cell carcinoma; N.D., not detected. *Linkage peak. #Candidate regions are based on MGI data.

to approximately 4.8 Mb by congenic mapping [61, 62]. As a result of an *in silico* search for a gene that is functionally dependent on the *p53* gene of *Stmm3*, *Cdkn2a* was extracted. The two tumor suppressor genes *p19^{Arf}* and *p16^{Ink4a}* are encoded by *Cdkn2a* through the sharing of exons, and both proteins have amino acid substitutions in one polymorphism between FVB/N and MSM/Ms. Based on these results, the most promising candidate gene for *Stmm3* was considered to be *Cdkn2a*.

On the other hand, there are 15 protein-encoding genes in *Stmm1a*, and their details are still under investigation. There were 28 protein-encoding genes in *Stmm1b*. *Pth* (parathyroid hormone) was extracted as a gene with an amino acid substitution between FVB/N and MSM/Ms. Therefore, we focused on *Pth* as one of the candidate genes for *Stmm1b*.

***Stmm1b*: Parathyroid Hormone is a Novel Regulator of Early-stage Skin Carcinogenesis**

PTH is a peptide hormone that, along with vitamin D, is essential for calcium homeostasis in the body [71, 72]. It is well known that the skin acts as a neuroendocrine organ. Almost all the elements controlling the hypothalamus-pituitary-adrenal axis activity are expressed in the skin, as previously described in detail [73]. PTH and PTH-related peptide (PTHrP) also influence the proliferation and differentiation of epidermal cells [74–77] via paracrine and intracrine routes [78], but the role of PTH in skin carcinogenesis is poorly understood. Surprisingly, a comparison of serum intact PTH (iPTH) between the two mouse strains showed that MSM/Ms had sig-

nificantly higher iPTH levels than FVB/N (5–10 times higher), while there was no difference in calcium and vitamin D levels [59]. Furthermore, the amount of iPTH in serum was approximately twice as high in *Stmm1b* sub-congenic mice compared with control mice [59].

According to a report by Kalu and Hardin, the basal circulating PTH level in sera is higher in rodents than in humans. Besides, there are differences between rodent strains, with the rat F344 strain having the highest PTH levels and the Wistar and Sprague Dawley rats having low PTH levels [79]. Therefore, differences in serum PTH levels, such as those seen between MSM/Ms and FVB/N, are also observed between and within species.

Next, a highly PTH-expressing *Pth^{MSM-Tg}* was prepared by introducing an MSM/Ms-BAC clone containing a *Pth* genetic region into FVB/N mice, and we then carried out a skin carcinogenesis experiment. The results showed that *Pth^{MSM-Tg}* was resistant to skin carcinogenesis. In addition, based on the results of carcinogenesis experiments using *Pth* heterozygous knockout mice (*Pth^{+/-}*), it was clarified that mice with low iPTH levels were susceptible to skin carcinogenesis, and it was possible to show for the first time that PTH is a skin cancer modifier (Fig. 3) [59].

We then detected a well-conserved Val/Met polymorphism (rs51104087) in the Pro-PTH region (amino acid position 28) of the mouse *Pth* gene, between FVB/N (i.e., valine) and MSM/Ms (i.e., methionine). The Pro-PTH sequence is conserved in mammals and is essential for the signal peptide sequence *in vitro* [80] and *in vivo* [81]. Based on a MoG+ database search, this cSNP in *Pth* exon 1 was found only in wild-derived strains and was well conserved in *musculus* subspecies (Table 2).

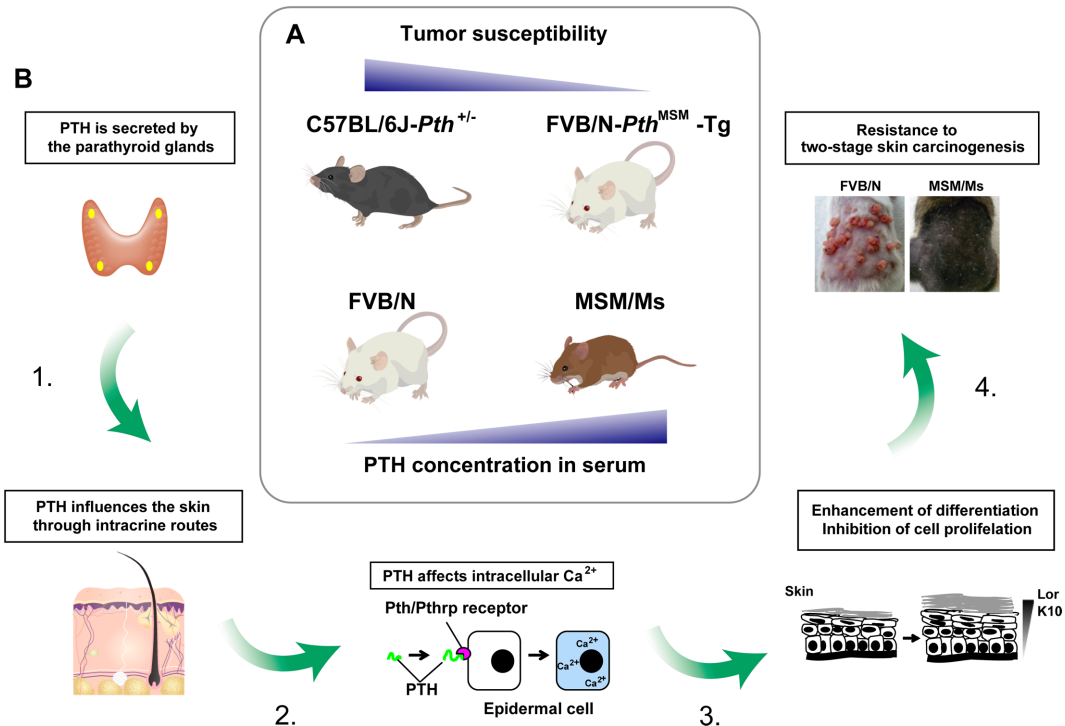


Fig. 3. A proposed model of the skin carcinogenesis-suppressing effect of circulating parathyroid hormone. (A) From the results of 7,12-dimethylbenz(a)anthracene (DMBA)/12-*O*-tetradecanoylphorbol-13-acetate (TPA) skin carcinogenesis experiments using genetically modified mice of PTH, FVB/N and MSM/Ms, it was clear that mice with high serum intact PTH levels are less susceptible to skin carcinogenesis. (B) 1. PTH is secreted from the parathyroid glands and acts on skin tissue via the endocrine routes. 2. PTH raises intracellular calcium in epidermal cells via Pth/Pthrp receptors. 3. Epidermal cells with elevated intracellular calcium promote differentiation and suppression of cell proliferation. 4. As a result, a high concentration of serum intact PTH leads to resistance to chemically induced skin carcinogenesis in MSM/Ms.

Table 2. Variant table for *Pth* and *p19^{Arf}* in wild-derived strain mice

wild-derived strains	Subspecies	<i>Pth</i> _rs51104087	PTH_amino acid 28	<i>Cdkn2a</i> _rs218801173	<i>p19Arf</i> _amino acid 149
CAST/EiJ	<i>castaneus</i>	G	Val	G	Val
HMI/Ms	<i>castaneus</i>	G	Val	G	Val
WSB/EiJ	<i>domesticus</i>	G	Val	C	Leu
BFM/2/Ms	<i>domesticus</i>	G	Val	C	Leu
PGN2/Ms	<i>domesticus</i>	G	Val	C	Leu
MOLF/EiJ	<i>molossinus</i>	G	Val	G	Val
JF1/Ms	<i>molossinus</i>	G	Val	G	Val
MSM/Ms	<i>molossinus</i>	A	Met	G	Val
CHD/Ms	<i>musculus</i>	G	Val	G	Val
PWK/PhJ	<i>musculus</i>	A	Met	G	Val
KJR/Ms	<i>musculus</i>	A	Met	G	Val
SWN/Ms	<i>musculus</i>	A	Met	G	Val
NJL/Ms	<i>musculus</i>	A	Met	G	Val
BLG2/Ms	<i>musculus</i>	A	Met	G	Val

Sequence data from MoG+.

We hypothesized that the cSNP in Pro-PTH could influence protein posttranslational modifications and increase secreted PTH levels. Nascent PTH is translated as a pre-pro protein. Thus, analysis of the effect of this SNP in *in vitro* experiments confirmed that the intracellular stability of PTH was improved, and the amount of extracellular secretion was increased [59]. It was also shown that secreted PTH acts to suppress skin cancer by

inducing the suppression of epidermal cell proliferation, an increase in intracellular calcium, and accompanying cell pro-differentiation, in a quantity-dependent manner (Fig. 3) [59].

These results showed that *Pth* accounts, at least in part, for the effects attributed to *Stmm1b*. Our data demonstrating the association between high serum PTH levels and skin tumor suppression in a two-stage skin

carcinogenesis model, underscore the potential therapeutic effect of using PTH or PTH analogs in skin cancer prevention and treatment.

***Stmm3*: Cdkn2a/p19^{Arf} Confers Resistance to Late-stage Papillomas and SCC by Activating the p53 Pathway**

In our previous report, we demonstrated a genome-wide significant linkage at *Stmm3* on chromosome 4. However, this linkage peak at *Stmm3* completely disap-

peared in *p53*^{+/-} mice. We concluded that corresponding genes for *Stmm3* are genetically dependent on *p53* [57, 61]. Next, we generated *p53*^{+/-} and *p53*^{+/+} sub-congenic mouse lines for *Stmm3*. These mice were exposed to two-stages of skin carcinogenesis using DMBA/TPA [62]. The skin carcinogenesis experiments revealed that both *p53*^{+/-}-*Stmm3*^{FVB/FVB} and *p53*^{+/-}-*Stmm3*^{FVB/MSM} mice developed late-stage (larger than 6 mm in diameter) papillomas (Fig. 4A). In contrast, when we measured the size of papillomas in *p53*^{+/+} sub-congenic mice, only *Stmm3*^{FVB/FVB} mice developed late-stage papillomas

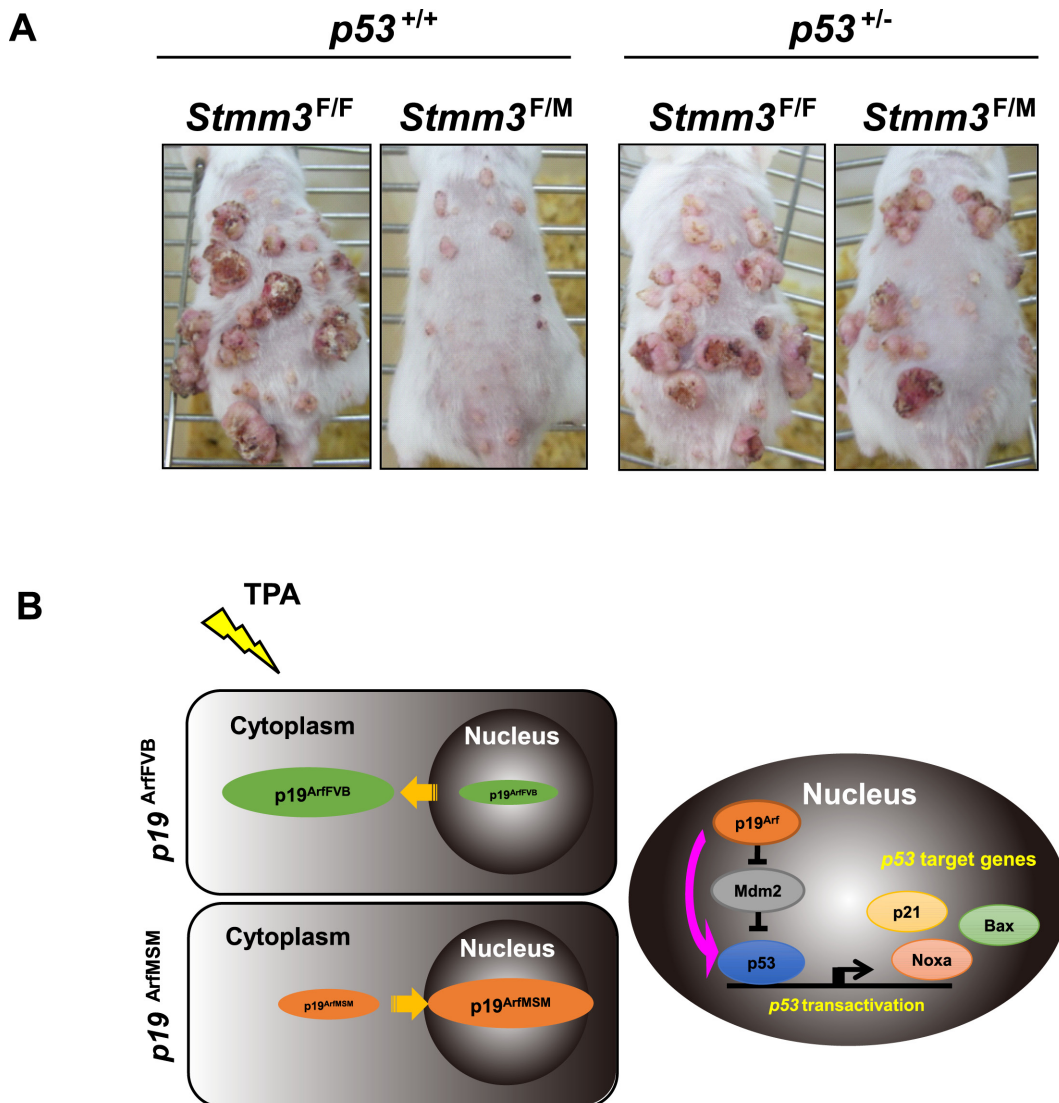


Fig. 4. *p19*^{ArfMSM} more efficiently induces the transcriptional activity of p53 compared with *p19*^{ArfFVB}. (A) Representative dorsal back skin photographs of *p53*^{+/+} or *p53*^{+/-}-*Stmm3*^{FVB/FVB} (*Stmm3*^{F/F}) and *Stmm3*^{FVB/MSM} (*Stmm3*^{F/M}) congenic mice at 20 weeks after 7,12-dimethylbenz (a) anthracene (DMBA)/12-*O*-tetradecanoylphorbol-13-acetate (TPA) initiation. (B) This figure shows the molecular mechanism behind the suppressive effect of *p19*^{ArfMSM} in late-stage papillomas. We noted that *p19*^{ArfMSM} was preferentially localized in the nucleus after TPA treatment. In contrast, *p19*^{ArfFVB} was preferentially localized in the cytoplasm. *p19*^{Arf} mediates p53 transactivation in the nucleus by stabilizing p53 protein through inactivation of Mdm2 protein. In addition, the nuclear localization of *p19*^{Arf} is necessary for this transactivation function. Eventually, *p19*^{ArfMSM} led to an increase in p53 stabilization and activated the p53 pathway. Therefore, we conclude that one of the responsible genes for *Stmm3* is *p19*^{Arf}.

(Fig. 4A). Therefore, the *Stmm3* region exerted more potent suppressive effects on papillomas in the presence of two copies of *p53*, indicating that the effects of *Stmm3* are dependent on the *p53* gene [62].

Based on congenic mapping results, we focused on *p53*-related *Cdkn2a* as a candidate factor for *Stmm3* [61]. Two tumor suppressor genes, *p19^{Arf}* and *p16^{Ink4a}*, are encoded by *Cdkn2a* through the sharing of exons. Therefore, each gene knockout mouse was prepared by genome editing with CRISPR/Cas9 using ES cells of MSM/Ms [62]. Furthermore, by mating these mice with FVB/N, MSM/Ms allele knockout mice with an F₁ genetic background were produced, and two-stage skin carcinogenesis experiments were performed. The results revealed *p19^{Arf}* to be the most promising candidate gene for *Stmm3*, as only MSM/Ms allele KO mice with *p19^{Arf}* showed significant increases in the number of late-stage benign tumors, the incidence of malignant tumors, and prolongation of mouse survival [62].

No significant difference was observed between the *p19^{Arf}* RNA expression levels and the *p19^{Arf}* protein levels between cutaneous tissues of the two mouse strains. On the other hand, the responsible SNP (rs218801173) between MSM/Ms (valine) and FVB/N (leucine) was localized in the C-terminal domain of *p19^{Arf}*. In addition, this SNP was not found in most inbred and wild-derived mice belonging to *M. m. domesticus* and was widely conserved in wild-derived mice not belonging to *M. m. domesticus* subspecies, including MSM/Ms (Table 2).

In cell localization experiments, deletion mutants lacking the C-terminal domain were wholly localized in the cytoplasm without entering the nucleus. Arf has been reported to be degraded, at least in part, by the proteasome in the cytoplasm [82, 83]. Thus, the C-terminal domain of *p19^{Arf}* may localize proteins in the nucleus to avoid degradation. However, human *p14^{ARF}* lacks this C-terminal region [84, 85]. Therefore, the biological importance of the C-terminal region may be overlooked.

When the SNP was introduced into 3T3 cells by retroviral transfection, it was found that stimulation of TPA resulted in a change in *p19^{Arf}* localization and that the MSM/MS allele would likely be localized in the nucleus (Fig. 4B). *p19^{Arf}* stabilizes *p53* protein by inactivating Mdm2 protein and mediating *p53* transactivation [86]. In addition, the nuclear localization of *p19^{Arf}* is necessary for this transactivation function [87, 88] (Fig. 4B). Therefore, we quantified the amount of *p53* protein and the expression level of downstream factors (such as *p21*, *Bax*, and *Noxa*) in mouse skin. The results showed that mice carrying the MSM/Ms allele had higher *p53* protein levels and elevated levels of downstream factor mRNA expression (Fig. 4B) [62].

We also revealed two SNPs of *CDKN2A* associated with breast cancer incidence in the Japanese cancer population. An SNP (rs36228836) in linkage disequilibrium with one of the two SNPs, was predicted by *in silico* analysis to affect transcription factor binding. This result suggests that rs36228836 influences breast cancer risk via transcriptional regulation. In recent years, SNPs near the *CDKN2A/B* locus on chromosome 9q21.3 have been linked to the risk of various human cancers and metabolic disorders [89].

We demonstrated that genetic polymorphisms in *Cdkn2a* and *CDKN2A* affect cancer risk. Therefore, we conclude that one of the genes responsible for *Stmm3* is *p19^{Arf}*. We have shown that linkage analysis using a mouse model can be translated to humans for identification of cancer susceptibility alleles and thus development of targeted therapies.

Concluding Remarks and Future Perspective

This review focused on the cancer susceptibility/resistance of a Japanese wild-derived inbred mouse strain, MSM/Ms, and attempted to identify the genetic modifiers. Forward genetics approaches have revealed that multiple genetic factors act on the two-stage process of skin carcinogenesis. In particular, it was shown that *Stmm1a/b* is involved in the development of early and mid-stage papillomas and that *Stmm3* functions in a *p53*-dependent manner in late-stage papillomas to SCCs.

To the best of our knowledge, this is the first to report that PTH, one of the genes responsible for *Stmm1b*, is involved in skin carcinogenesis. Additionally, the cSNP responsible for increased iPTH in sera may be derived from the *M. m. musculus* subspecies (Table 2). In the future, it will be essential to measure iPTH levels in some wild-derived mouse strains to determine their associations with a variety of diseases, including cancer. It is also necessary to clarify why MSM/Ms mice can maintain normal calcium and vitamin D levels despite high serum iPTH. Moreover, we are currently investigating associations with the incidences of several cancers as well as data for SNPs around PTH locus data in human cancer patients. In conjunction with this, we are verifying findings with mouse models other than skin carcinogenesis models using *Pth* knockout mice.

On the other hand, the SNP in the rodent-specific C-terminal region of *p19^{Arf}*, the gene we identified as being responsible for *Stmm3*, is a domain that has not been investigated in detail because it does not exist in humans. However, our research suggests that this domain is essential for the nuclear localization of *p19^{Arf}*, which may

shed light on the evolutionary properties and unknown functions of p19^{Arf} in other mammals. Further research is needed in the future. We are currently analyzing the gene responsible for *Stmm1a*, which has the most potent resistance effect, and we believe that identification of it will provide valuable insights into the cancer resistance in MSM/Ms.

In future studies, it will be essential to analyze human cancer susceptibility genes and polymorphisms by utilizing this information and integrating it with information from human GWAS. In addition, wild-derived inbred mice exhibit phenotypes different from those of classical strained mice for various genetic diseases [16, 90–92]. We are currently screening resistant candidate SNPs from haplotype analysis of wild-derived strain of mice based on *Stmm* candidate region information using a bioinformatics approach. We plan to introduce these candidate SNPs directly into susceptible inbred mice by CRISPR/Cas9 to perform carcinogenesis experiments and single-cell RNA sequencing. In the future, further technological innovations in areas such as sequencing and genome editing will clarify the cause of genetic diseases at the individual level, and it is thought that wild-derived inbred mouse strains will become an increasingly important and valuable genetic resource.

Acknowledgments

We would like to thank Dr. Ryo Kominami, Dr. Shigeharu Wakana, Mr. Ikuo Miura, Dr. Yuki Miyasaka, Dr. Eriko Isogai, Mr. Yasuhiro Yoshizawa, Ms. Miho Sato, Dr. Hiroshi Shitara, Ms. Midori Yamaguchi, Dr. Choji Taya, and Dr. Kimi Araki for their invaluable help with our research. We also sincerely thank Dr. Yoshiaki Kikawa for recommending the Young Investigator Award of Japanese Association for Laboratory Animal Science (JALAS). Some mouse and tissue illustrations in Fig. 2A and 3 were obtained from DBCLS TogoTV (<https://togotv.dbcls.jp/>). This work was supported by JSPS KAKENHI Grant numbers JP15K06817, JP19K07494 and JP16H06276 (AdAMS).

References

- Balmain A. Cancer as a complex genetic trait: tumor susceptibility in humans and mouse models. *Cell*. 2002; 108: 145–152. [Medline] [CrossRef]
- Balmain A, Gray J, Ponder B. The genetics and genomics of cancer. *Nat Genet*. 2003; 33:(Suppl): 238–244. [Medline] [CrossRef]
- Dietrich WF, Lander ES, Smith JS, Moser AR, Gould KA, Luongo C, et al. Genetic identification of Mom-1, a major modifier locus affecting Min-induced intestinal neoplasia in the mouse. *Cell*. 1993; 75: 631–639. [Medline] [CrossRef]
- Fijneman RJ, de Vries SS, Jansen RC, Demant P. Complex interactions of new quantitative trait loci, Sluc1, Sluc2, Sluc3, and Sluc4, that influence the susceptibility to lung cancer in the mouse. *Nat Genet*. 1996; 14: 465–467. [Medline] [CrossRef]
- Ruivenkamp CA, van Wezel T, Zanon C, Stassen AP, Vlcek C, Csikós T, et al. Ptpnj is a candidate for the mouse colon-cancer susceptibility locus Scc1 and is frequently deleted in human cancers. *Nat Genet*. 2002; 31: 295–300. [Medline] [CrossRef]
- Demant P. Cancer susceptibility in the mouse: genetics, biology and implications for human cancer. *Nat Rev Genet*. 2003; 4: 721–734. [Medline] [CrossRef]
- Dragani TA. 10 years of mouse cancer modifier loci: human relevance. *Cancer Res*. 2003; 63: 3011–3018. [Medline]
- Mao JH, Balmain A. Genomic approaches to identification of tumour-susceptibility genes using mouse models. *Curr Opin Genet Dev*. 2003; 13: 14–19. [Medline] [CrossRef]
- Kemp CJ. Multistep skin cancer in mice as a model to study the evolution of cancer cells. *Semin Cancer Biol*. 2005; 15: 460–473. [Medline] [CrossRef]
- Abel EL, Angel JM, Kiguchi K, DiGiovanni J. Multi-stage chemical carcinogenesis in mouse skin: fundamentals and applications. *Nat Protoc*. 2009; 4: 1350–1362. [Medline] [CrossRef]
- Okumura K, Saito M, Isogai E, Aoto Y, Hachiya T, Sakakibara Y, et al. Meis1 regulates epidermal stem cells and is required for skin tumorigenesis. *PLoS One*. 2014; 9: e102111. [Medline] [CrossRef]
- Okumura K, Kagawa N, Saito M, Yoshizawa Y, Munakata H, Isogai E, et al. CENP-R acts bilaterally as a tumor suppressor and as an oncogene in the two-stage skin carcinogenesis model. *Cancer Sci*. 2017; 108: 2142–2148. [Medline] [CrossRef]
- Aoto Y, Hachiya T, Okumura K, Hase S, Sato K, Wakabayashi Y, et al. DEClust: A statistical approach for obtaining differential expression profiles of multiple conditions. *PLoS One*. 2017; 12: e0188285. [Medline] [CrossRef]
- Aoto Y, Okumura K, Hachiya T, Hase S, Wakabayashi Y, Ishikawa F, et al. Time-Series Analysis of Tumorigenesis in a Murine Skin Carcinogenesis Model. *Sci Rep*. 2018; 8: 12994. [Medline] [CrossRef]
- Saito M, Kagawa N, Okumura K, Munakata H, Isogai E, Fukagawa T, et al. CENP-50 is required for papilloma development in the two-stage skin carcinogenesis model. *Cancer Sci*. 2020; 111: 2850–2860. [Medline] [CrossRef]
- Poltorak A, Apalko S, Sherbak S. Wild-derived mice: from genetic diversity to variation in immune responses. *Mamm Genome*. 2018; 29: 577–584. [Medline] [CrossRef]
- Conner JR, Smirnova II, Poltorak A. Forward genetic analysis of Toll-like receptor responses in wild-derived mice reveals a novel antiinflammatory role for IRAK1BP1. *J Exp Med*. 2008; 205: 305–314. [Medline] [CrossRef]
- Ashman LK, Murray AW, Cook MG, Kotlarski I. Two-stage skin carcinogenesis in sensitive and resistant mouse strains. *Carcinogenesis*. 1982; 3: 99–102. [Medline] [CrossRef]
- Bangrazi C, Mouton D, Neveu T, Saran A, Covelli V, Doria G, et al. Genetics of chemical carcinogenesis. 1. Bidirectional selective breeding of susceptible and resistant lines of mice to two-stage skin carcinogenesis. *Carcinogenesis*. 1990; 11: 1711–1719. [Medline] [CrossRef]
- Angel JM, Beltrán L, Minda K, Rupp T, DiGiovanni J. Association of a murine chromosome 9 locus (Psl1) with susceptibility to mouse skin tumor promotion by 12-O-tetradecanoylphorbol-13-acetate. *Mol Carcinog*. 1997; 20: 162–167. [Medline] [CrossRef]
- Angel JM, Caballero M, DiGiovanni J. Identification of novel genetic loci contributing to 12-O-tetradecanoylphorbol-13-acetate skin tumor promotion susceptibility in DBA/2 and C57BL/6 mice. *Cancer Res*. 2003; 63: 2747–2751. [Medline]
- Fujiwara K, Igarashi J, Irahara N, Kimura M, Nagase H. New chemically induced skin tumour susceptibility loci identified in a mouse backcross between FVB and dominant resistant

- PWK. *BMC Genet.* 2007; 8: 39. [Medline] [CrossRef]
23. Fujiwara K, Wie B, Elliott R, Nagase H. New outbred colony derived from *Mus musculus castaneus* to identify skin tumor susceptibility loci. *Mol Carcinog.* 2010; 49: 653–661. [Medline] [CrossRef]
 24. Fujiwara K, Inagaki Y, Soma M, Ozaki T, Nagase H. Mapping of new skin tumor susceptibility loci by a phenotype-driven congenic approach. *Oncol Lett.* 2018; 16: 6670–6676. [Medline]
 25. Nagase H, Bryson S, Cordell H, Kemp CJ, Fee F, Balmain A. Distinct genetic loci control development of benign and malignant skin tumours in mice. *Nat Genet.* 1995; 10: 424–429. [Medline] [CrossRef]
 26. Nagase H, Mao JH, Balmain A. A subset of skin tumor modifier loci determines survival time of tumor-bearing mice. *Proc Natl Acad Sci USA.* 1999; 96: 15032–15037. [Medline] [CrossRef]
 27. Peissel B, Zaffaroni D, Zanesi N, Zedda I, Manenti G, Rebessi S, et al. Linkage disequilibrium and haplotype mapping of a skin cancer susceptibility locus in outbred mice. *Mamm Genome.* 2000; 11: 979–981. [Medline] [CrossRef]
 28. Santos J, Montagutelli X, Acevedo A, López P, Vaquero C, Fernández M, et al. A new locus for resistance to gamma-radiation-induced thymic lymphoma identified using inter-specific consomic and inter-specific recombinant congenic strains of mice. *Oncogene.* 2002; 21: 6680–6683. [Medline] [CrossRef]
 29. To MD, Perez-Losada J, Mao JH, Hsu J, Jacks T, Balmain A. A functional switch from lung cancer resistance to susceptibility at the *Pas1* locus in *Kras2LA2* mice. *Nat Genet.* 2006; 38: 926–930. [Medline] [CrossRef]
 30. Wakabayashi Y, Mao JH, Brown K, Girardi M, Balmain A. Promotion of Hras-induced squamous carcinomas by a polymorphic variant of the *Patched* gene in FVB mice. *Nature.* 2007; 445: 761–765. [Medline] [CrossRef]
 31. Ewart-Toland A, Briassouli P, de Koning JP, Mao JH, Yuan J, Chan F, et al. Identification of *Stk6/STK15* as a candidate low-penetrance tumor-susceptibility gene in mouse and human. *Nat Genet.* 2003; 34: 403–412. [Medline] [CrossRef]
 32. Ha NH, Long J, Cai Q, Shu XO, Hunter KW. The Circadian Rhythm Gene *Arntl2* Is a Metastasis Susceptibility Gene for Estrogen Receptor-Negative Breast Cancer. *PLoS Genet.* 2016; 12: e1006267. [Medline] [CrossRef]
 33. Kawasaki K, Freimuth J, Meyer DS, Lee MM, Tochimoto-Okamoto A, Benzinou M, et al. Genetic variants of *Adam17* differentially regulate TGF β signaling to modify vascular pathology in mice and humans. *Proc Natl Acad Sci USA.* 2014; 111: 7723–7728. [Medline] [CrossRef]
 34. Moriwaki K, Miyashita N, Mita A, Gotoh H, Tsuchiya K, Kato H, et al. Unique inbred strain MSM/Ms established from the Japanese wild mouse. *Exp Anim.* 2009; 58: 123–134. [Medline] [CrossRef]
 35. Takada T, Ebata T, Noguchi H, Keane TM, Adams DJ, Narita T, et al. The ancestor of extant Japanese fancy mice contributed to the mosaic genomes of classical inbred strains. *Genome Res.* 2013; 23: 1329–1338. [Medline] [CrossRef]
 36. Takada T, Yoshiki A, Obata Y, Yamazaki Y, Shiroishi T. NIG_MoG: a mouse genome navigator for exploring interspecific genetic polymorphisms. *Mamm Genome.* 2015; 26: 331–337. [Medline] [CrossRef]
 37. Takada T, Mita A, Maeno A, Sakai T, Shitara H, Kikkawa Y, et al. Mouse inter-subspecific consomic strains for genetic dissection of quantitative complex traits. *Genome Res.* 2008; 18: 500–508. [Medline] [CrossRef]
 38. Abe K, Noguchi H, Tagawa K, Yuzuriha M, Toyoda A, Kojima T, et al. Contribution of Asian mouse subspecies *Mus musculus molossinus* to genomic constitution of strain C57BL/6J, as defined by BAC-end sequence-SNP analysis. *Genome Res.* 2004; 14: 2439–2447. [Medline] [CrossRef]
 39. Kikkawa Y, Miura I, Takahama S, Wakana S, Yamazaki Y, Moriwaki K, et al. Microsatellite database for MSM/Ms and JF1/Ms, molossinus-derived inbred strains. *Mamm Genome.* 2001; 12: 750–752. [Medline] [CrossRef]
 40. Araki K, Takeda N, Yoshiki A, Obata Y, Nakagata N, Shiroishi T, et al. Establishment of germline-competent embryonic stem cell lines from the MSM/Ms strain. *Mamm Genome.* 2009; 20: 14–20. [Medline] [CrossRef]
 41. Nakahara M, Tateyama H, Araki M, Nakagata N, Yamamura K, Araki K. Gene-trap mutagenesis using Mol/MSM-1 embryonic stem cells from MSM/Ms mice. *Mamm Genome.* 2013; 24: 228–239. [Medline] [CrossRef]
 42. Pataer A, Kamoto T, Lu LM, Yamada Y, Hiai H. Two dominant host resistance genes to pre-B lymphoma in wild-derived inbred mouse strain MSM/Ms. *Cancer Res.* 1996; 56: 3716–3720. [Medline]
 43. Okumoto M, Mori N, Miyashita N, Moriwaki K, Imai S, Haga S, et al. Radiation-induced lymphomas in MSM, (BALB/cHeA x MSM) F1 and (BALB/cHeA x STS/A) F1 hybrid mice. *Exp Anim.* 1995; 44: 43–48. [Medline] [CrossRef]
 44. Matsumoto Y, Kosugi S, Shinbo T, Chou D, Ohashi M, Wakabayashi Y, et al. Allelic loss analysis of gamma-ray-induced mouse thymic lymphomas: two candidate tumor suppressor gene loci on chromosomes 12 and 16. *Oncogene.* 1998; 16: 2747–2754. [Medline] [CrossRef]
 45. Okamoto M, Yonekawa H. Intestinal tumorigenesis in Min mice is enhanced by X-irradiation in an age-dependent manner. *J Radiat Res (Tokyo).* 2005; 46: 83–91. [Medline] [CrossRef]
 46. Nemoto M, Morita Y, Mishima Y, Takahashi S, Nomura T, Ushiki T, et al. *Ahl3*, a third locus on mouse chromosome 17 affecting age-related hearing loss. *Biochem Biophys Res Commun.* 2004; 324: 1283–1288. [Medline] [CrossRef]
 47. Morita Y, Hirokawa S, Kikkawa Y, Nomura T, Yonekawa H, Shiroishi T, et al. Fine mapping of *Ahl3* affecting both age-related and noise-induced hearing loss. *Biochem Biophys Res Commun.* 2007; 355: 117–121. [Medline] [CrossRef]
 48. Kikkawa Y, Seki Y, Okumura K, Ohshiba Y, Miyasaka Y, Suzuki S, et al. Advantages of a mouse model for human hearing impairment. *Exp Anim.* 2012; 61: 85–98. [Medline] [CrossRef]
 49. Miyasaka Y, Shitara H, Suzuki S, Yoshimoto S, Seki Y, Ohshiba Y, et al. Heterozygous mutation of *Ush1g/Sans* in mice causes early-onset progressive hearing loss, which is recovered by reconstituting the strain-specific mutation in *Cdh23*. *Hum Mol Genet.* 2016; 25: 2045–2059. [Medline] [CrossRef]
 50. Yasuda SP, Seki Y, Suzuki S, Ohshiba Y, Hou X, Matsuoka K, et al. c.753A>G genome editing of a *Cdh23^{abl}* allele delays age-related hearing loss and degeneration of cochlear hair cells in C57BL/6J mice. *Hear Res.* 2020; 389: 107926. [Medline] [CrossRef]
 51. Takahashi A, Shiroishi T, Koide T. Multigenic factors associated with a hydrocephalus-like phenotype found in inter-subspecific consomic mouse strains. *Mamm Genome.* 2008; 19: 333–338. [Medline] [CrossRef]
 52. Takahashi A, Tomihara K, Shiroishi T, Koide T. Genetic mapping of social interaction behavior in B6/MSM consomic mouse strains. *Behav Genet.* 2010; 40: 366–376. [Medline] [CrossRef]
 53. Nishi A, Ishii A, Takahashi A, Shiroishi T, Koide T. QTL analysis of measures of mouse home-cage activity using B6/MSM consomic strains. *Mamm Genome.* 2010; 21: 477–485. [Medline] [CrossRef]
 54. Arakawa T, Tanave A, Ikeuchi S, Takahashi A, Kakihara S, Kimura S, et al. A male-specific QTL for social interaction behavior in mice mapped with automated pattern detection by a hidden Markov model incorporated into newly developed freeware. *J Neurosci Methods.* 2014; 234: 127–134. [Medline] [CrossRef]
 55. Takahashi A, Shiroishi T, Koide T. Genetic mapping of escalated aggression in wild-derived mouse strain MSM/Ms: association with serotonin-related genes. *Front Neurosci.* 2014;

- 8: 156. [Medline] [CrossRef]
56. Takahashi A, Sugimoto H, Kato S, Shiroishi T, Koide T. Mapping of Genetic Factors That Elicit Intermale Aggressive Behavior on Mouse Chromosome 15: Intruder Effects and the Complex Genetic Basis. *PLoS One*. 2015; 10: e0137764. [Medline] [CrossRef]
 57. Okumura K, Sato M, Saito M, Miura I, Wakana S, Mao JH, et al. Independent genetic control of early and late stages of chemically induced skin tumors in a cross of a Japanese wild-derived inbred mouse strain, MSM/Ms. *Carcinogenesis*. 2012; 33: 2260–2268. [Medline] [CrossRef]
 58. Okumura K, Saito M, Isogai E, Miura I, Wakana S, Kominami R, et al. Congenic mapping and allele-specific alteration analysis of *Stmm1* locus conferring resistance to early-stage chemically induced skin papillomas. *PLoS One*. 2014; 9: e97201. [Medline] [CrossRef]
 59. Okumura K, Saito M, Yoshizawa Y, Munakata H, Isogai E, Miura I, et al. The parathyroid hormone regulates skin tumour susceptibility in mice. *Sci Rep*. 2017; 7: 11208. [Medline] [CrossRef]
 60. Saito M, Okumura K, Miura I, Wakana S, Kominami R, Wakabayashi Y. Identification of *Stmm3* locus conferring resistance to late-stage chemically induced skin papillomas on mouse chromosome 4 by congenic mapping and allele-specific alteration analysis. *Exp Anim*. 2014; 63: 339–348. [Medline] [CrossRef]
 61. Saito M, Okumura K, Isogai E, Araki K, Tanikawa C, Matsuda K, et al. A Polymorphic Variant in *p19^{Arf}* Confers Resistance to Chemically Induced Skin Tumors by Activating the p53 Pathway. *J Invest Dermatol*. 2019; 139: 1459–1469. [Medline] [CrossRef]
 62. Manenti G, Binelli G, Gariboldi M, Canzian F, De Gregorio L, Falvella FS, et al. Multiple loci affect genetic predisposition to hepatocarcinogenesis in mice. *Genomics*. 1994; 23: 118–124. [Medline] [CrossRef]
 63. Kodama Y, Yoshikai Y, Tamura Y, Wakana S, Takagi R, Niwa O, et al. The *D5Mit7* locus on mouse chromosome 5 provides resistance to gamma-ray-induced but not N-methyl-N-nitrosourea-induced thymic lymphomas. *Carcinogenesis*. 2004; 25: 143–148. [Medline] [CrossRef]
 64. Darakhshan F, Badie C, Moody J, Coster M, Finnon R, Finnon P, et al. Evidence for complex multigenic inheritance of radiation AML susceptibility in mice revealed using a surrogate phenotypic assay. *Carcinogenesis*. 2006; 27: 311–318. [Medline] [CrossRef]
 65. Hiai H, Abujiang P, Nishimura M. Polygenic resistance to mouse pulmonary adenomas. *Exp Lung Res*. 2000; 26: 617–625. [Medline] [CrossRef]
 66. Festing MF, Lin L, Devereux TR, Gao F, Yang A, Anna CH, et al. At least four loci and gender are associated with susceptibility to the chemical induction of lung adenomas in A/J x BALB/c mice. *Genomics*. 1998; 53: 129–136. [Medline] [CrossRef]
 67. Manenti G, Gariboldi M, Elango R, Fiorino A, De Gregorio L, Falvella FS, et al. Genetic mapping of a pulmonary adenoma resistance (*Par1*) in mouse. *Nat Genet*. 1996; 12: 455–457. [Medline] [CrossRef]
 68. Wang M, Zhang Z, Zhang Z, Vikis H, Yan Y, Wang Y, et al. Fine mapping and candidate gene analyses of pulmonary adenoma resistance 1, a major genetic determinant of mouse lung adenoma resistance. *Cancer Res*. 2007; 67: 2508–2516. [Medline] [CrossRef]
 69. Wang Y, Zhang Z, Yan Y, Lemon WJ, LaRegina M, Morrison C, et al. A chemically induced model for squamous cell carcinoma of the lung in mice: histopathology and strain susceptibility. *Cancer Res*. 2004; 64: 1647–1654. [Medline] [CrossRef]
 70. de Koning JP, Wakabayashi Y, Nagase H, Mao JH, Balmain A. Convergence of congenic mapping and allele-specific alterations in tumors for the resolution of the *Skts1* skin tumor susceptibility locus. *Oncogene*. 2007; 26: 4171–4178. [Medline] [CrossRef]
 71. Miao D, He B, Lanske B, Bai XY, Tong XK, Hendy GN, et al. Skeletal abnormalities in Pth-null mice are influenced by dietary calcium. *Endocrinology*. 2004; 145: 2046–2053. [Medline] [CrossRef]
 72. Xue Y, Karaplis AC, Hendy GN, Goltzman D, Miao D. Genetic models show that parathyroid hormone and 1,25-dihydroxyvitamin D3 play distinct and synergistic roles in postnatal mineral ion homeostasis and skeletal development. *Hum Mol Genet*. 2005; 14: 1515–1528. [Medline] [CrossRef]
 73. Slominski A, Wortsman J. Neuroendocrinology of the skin. *Endocr Rev*. 2000; 21: 457–487. [Medline]
 74. Holick MF, Ray S, Chen TC, Tian X, Persons KS. A parathyroid hormone antagonist stimulates epidermal proliferation and hair growth in mice. *Proc Natl Acad Sci USA*. 1994; 91: 8014–8016. [Medline] [CrossRef]
 75. Safer JD, Ray S, Holick MF. A topical parathyroid hormone/parathyroid hormone-related peptide receptor antagonist stimulates hair growth in mice. *Endocrinology*. 2007; 148: 1167–1170. [Medline] [CrossRef]
 76. Peters EM, Foitzik K, Paus R, Ray S, Holick MF. A new strategy for modulating chemotherapy-induced alopecia, using PTH/PTHrP receptor agonist and antagonist. *J Invest Dermatol*. 2001; 117: 173–178. [Medline] [CrossRef]
 77. Wysolmerski JJ, Broadus AE, Zhou J, Fuchs E, Milstone LM, Philbrick WM. Overexpression of parathyroid hormone-related protein in the skin of transgenic mice interferes with hair follicle development. *Proc Natl Acad Sci USA*. 1994; 91: 1133–1137. [Medline] [CrossRef]
 78. Skrok A, Bednarczuk T, Skwarek A, Popow M, Rudnicka L, Olszewska M. The effect of parathyroid hormones on hair follicle physiology: implications for treatment of chemotherapy-induced alopecia. *Skin Pharmacol Physiol*. 2015; 28: 213–225. [Medline] [CrossRef]
 79. Kalu DN, Hardin RR. Age, strain and species differences in circulating parathyroid hormone. *Horm Metab Res*. 1984; 16: 654–657. [Medline] [CrossRef]
 80. Wren KM, Potts JT Jr, Kronenberg HM. Importance of the propeptide sequence of human preproparathyroid hormone for signal sequence function. *J Biol Chem*. 1988; 263: 19771–19777. [Medline] [CrossRef]
 81. Adriaansen J, Zheng C, Perez P, Baum BJ. Production and sorting of transgenic, modified human parathyroid hormone in vivo in rat salivary glands. *Biochem Biophys Res Commun*. 2010; 391: 768–772. [Medline] [CrossRef]
 82. Inoue R, Shiraiishi T. PKC α is involved in phorbol ester TPA-mediated stabilization of p14ARF. *Biochem Biophys Res Commun*. 2005; 330: 1314–1318. [Medline] [CrossRef]
 83. Vivo M, Ranieri M, Sansone F, Santoriello C, Calogero RA, Calabrò V, et al. Mimicking p14ARF phosphorylation influences its ability to restrain cell proliferation. *PLoS One*. 2013; 8: e53631. [Medline] [CrossRef]
 84. Maggi LB Jr, Winkler CL, Miceli AP, Apicelli AJ, Brady SN, Kuchenreuther MJ, et al. ARF tumor suppression in the nucleolus. *Biochim Biophys Acta*. 2014; 1842: 831–839. [Medline] [CrossRef]
 85. Quelle DE, Cheng M, Ashmun RA, Sherr CJ. Cancer-associated mutations at the *INK4a* locus cancel cell cycle arrest by p16^{INK4a} but not by the alternative reading frame protein p19^{ARF}. *Proc Natl Acad Sci USA*. 1997; 94: 669–673. [Medline] [CrossRef]
 86. Kamijo T, Weber JD, Zambetti G, Zindy F, Roussel MF, Sherr CJ. Functional and physical interactions of the ARF tumor suppressor with p53 and Mdm2. *Proc Natl Acad Sci USA*. 1998; 95: 8292–8297. [Medline] [CrossRef]
 87. Gannon JV, Lane DP. Protein synthesis required to anchor a mutant p53 protein which is temperature-sensitive for nuclear transport. *Nature*. 1991; 349: 802–806. [Medline] [CrossRef]
 88. Shaulsky G, Goldfinger N, Tosky MS, Levine AJ, Rotter V.

- Nuclear localization is essential for the activity of p53 protein. *Oncogene*. 1991; 6: 2055–2065. [[Medline](#)]
89. Kong Y, Sharma RB, Ly S, Stamateris RE, Jesdale WM, Alonso LC. *CDKN2A/B* T2D Genome-Wide Association Study Risk SNPs Impact Locus Gene Expression and Proliferation in Human Islets. *Diabetes*. 2018; 67: 872–884. [[Medline](#)] [[CrossRef](#)]
 90. Wada K, Yasuda SP, Kikkawa Y. Genetic modifiers of rodent animal models: the role in cataractogenesis. *Exp Anim*. 2019; 68: 397–406. [[Medline](#)] [[CrossRef](#)]
 91. Chang PL, Kopania E, Keeble S, Sarver BAJ, Larson E, Orth A, et al. Whole exome sequencing of wild-derived inbred strains of mice improves power to link phenotype and genotype. *Mamm Genome*. 2017; 28: 416–425. [[Medline](#)] [[CrossRef](#)]
 92. Matsushima Y. Japanese wild mice: a rich resource for new disease models. *Exp Anim*. 2012; 61: 25–33. [[Medline](#)] [[CrossRef](#)]